Journal of Power Sources 273 (2015) 1056–1064

Contents lists available at ScienceDirect

Journal of Power Sources

journal homepage: www.elsevier.com/locate/jpowsour

Survey of the transport properties of sodium superionic conductor materials for use in sodium batteries

M. Guin, F. Tietz*

Forschungszentrum Jülich GmbH, Institute of Energy and Climate Research (IEK-1), D-52425 Jülich, Germany

HIGHLIGHTS

- Extensive study of ionic conductivity of all Na-containing NASICON materials.
- The optimal size for the transition metal cations is 0.72 Å.
- Maximum conductivity with 3.3 mol Na per formula unit and monoclinic distortion.
- Impact of structural bottleneck for sodium conduction was validated.

ARTICLE INFO

Article history:
Received 31 July 2014
Received in revised form
5 September 2014
Accepted 21 September 2014
Available online 28 September 2014

Keywords:
Ionic conductivity
NASICON
Sodium
Sodium batteries

ABSTRACT

One important issue in future scenarios predominantly using renewable energy sources is the electrochemical storage of electricity in batteries. Among all rechargeable battery technologies, Li-ion cells have the largest energy density and output voltage today, but they have yet to be optimized in terms of capacity, safety and cost for use as stationary systems. Recently, sodium batteries have been attracting attention again because of the abundant availability of Na. However, much work is still required in the field of sodium batteries in order to mature this technology.

Sodium superionic conductor (NASICON) materials are a thoroughly studied class of solid electrolytes. In this study, their crystal structure, compositional diversity and ionic conductivity are surveyed and analysed in order to correlate the lattice parameters and specific crystal structure data with sodium conductivity and activation energy using as much data sets as possible. Approximately 110 compositions with the general formula $Na_{1+2w+x-y+z}M_w^{(II)}M_x^{(III)}M_y^{(V)}M_{2-w-x-y}^{(IV)}(SiO_4)_z(PO_4)_{3-z}$ were included in the data collection to determine an optimal size for the M cations. In addition, the impact of the amount of Na per formula unit on the conductivity and the substitution of P with Si are discussed. An extensive study of the size of the structural bottleneck for sodium conduction (formed by triangles of oxygen ions) was carried out to validate the influence of this geometrical parameter on sodium conductivity.

1. Introduction

The environmental concerns about the use of fossil fuels and their resource constraints have led to a great interest in renewable energy sources. Solar and wind energy are among the most abundant and potentially available sources, but they do not deliver a regular supply that can be easily adjusted in response to demand and are therefore not reliable sources of power [1]. New electrical energy storage is crucial, as it will allow energy to be stored during peak hours and released when it is needed.

Some known energy storage systems cannot be used on a large scale because of their costs or their availability (pumped hydro storage, superconducting magnetic energy storage, compressed air energy storage) [2]. Other systems are under development (hydrogen storage with fuel cells, thermal energy storage). Among existing storage systems, the most promising solution is electrochemical storage. In this storage solution, batteries provide stored chemical energy with the ability to convert it as electrical energy with high efficiency. Among all commercially available and rechargeable batteries today, Li-ion cells have the largest energy density and output voltage. However, for stationary battery systems, the requirements of high capacity, high safety, long lifetime and low cost need to be addressed in a different way than for consumer electronics or electromobility. Hence, Na-based

* Corresponding author. Tel.: +49 2461 61 5007; fax: +49 2461 61 2455.
E-mail address: f.tietz@fz-juelich.de (F. Tietz).

http://dx.doi.org/10.1016/j.jpowsour.2014.09.137
0378-7753/

compounds have recently made a comeback because the costs of Li are set to rise strongly as the resource availability decreases [3].

The search for commercially viable Na or Na-ion batteries is based on finding and optimizing new electrode materials and electrolytes. Na battery systems are not new and some have already been commercialized, such as the sodium sulphur (Na–S) and ZEBRA cells which are based on Na–$NiCl_2$ [4]. Both types of cells operate at high temperature (near 300 °C) where sodium and the positive electrodes are molten. The electrolyte is β-alumina ($NaAl_{11}O_{17}$), which was discovered nearly 80 years ago [5]. Other fast sodium-ion conductors have been under development in recent years (manganese oxides [6,7], layered oxides [8], NASICON materials [9], olivines [10,11], fluorophosphates [12,13,14]). They have pushed this field forward and led to the possibility of Na batteries that operate at lower temperatures, i.e. either at room temperature or just above the melting point of sodium (100 °C). Particularly for stationary applications like the back-up storage of renewable energy previously mentioned, the constraint of operation temperature can be regarded as less demanding than for other applications.

In this study, we concentrate on NASICON materials (***Na***$^+$ ***s***uper***i***onic ***con***ductors). For 40 years, they have been a thoroughly studied class of sodium-ion conductors that can be used as a solid electrolyte in Na-ion batteries as demonstrated for the first time by Lalère et al. [15]. This present study summarizes the available published data on crystal structure, compositions and ionic conductivity in order to generate structure-composition-property relationships, i.e. to correlate the lattice parameters and specific crystal structure data with sodium mobility and the activation energy of ionic conduction.

2. NASICON materials: definition and compositional diversity

NASICON materials were mentioned for the first time in the reports of Hong and Goodenough from 1976 [9,16] on the synthesis and characterization of $Na_{1+x}Zr_2Si_xP_{3-x}O_{12}$ ($0 \le x \le 3$). This meanwhile popular abbreviation is used for phosphates with the generic formula AMP_3O_{12}. In this family of compositions a wide variation of substitutions have been reported and are reviewed in Ref. [17]. The A-site can be occupied by

- monovalent cations: Li^+, Na^+, K^+, Rb^+, Cs^+, H^+, H_3O^+, NH^{4+}, Cu^+, Ag^+,
- divalent cations: Mg^{2+}, Ca^{2+}, Sr^{2+}, Ba^{2+}, Cu^{2+}, Pb^{2+},Cd^{2+}, Mn^{2+}, Co^{2+}, Ni^{2+}, Zn^{2+},
- trivalent cations: Al^{3+}, Y^{3+}, La^{3+}–Lu^{3+},
- tetravalent cations: Ge^{4+}, Zr^{4+}, Hf^{4+}

Or it can also be vacant in the case that the M-site is occupied by pentavalent cations. The M sites can be occupied by

- divalent cations: Cd^{2+}, Mn^{2+}, Co^{2+}, Ni^{2+}, Zn^{2+},
- trivalent cations: Al^{3+}, Ga^{3+}, In^{3+}, Sc^{3+}, Ti^{3+}, V^{3+}, Cr^{3+}, Fe^{3+}, Y^{3+}, La^{3+}–Lu^{3+},
- tetravalent cations: Si^{4+}, Ge^{4+}, Sn^{4+}, Ti^{4+}, Zr^{4+}, Hf^{4+}, V^{4+}, Nb^{4+}, Mo^{4+}, and
- pentavalent cations: V^{5+}, Nb^{5+}, Ta^{5+}, Sb^{5+}, As^{5+}

to balance the charge suitably. In addition, phosphorus has been partially substituted by Si, Ge or As. In the following, only compositions with sodium ions are considered, particularly those with the extended general formula $Na_{1+2w+x-y+z}M_w^{(II)}M_x^{(III)}M_y^{(V)}M_{2-w-x-y}^{(IV)}(SiO_4)_z(PO_4)_{3-z}$. However, the structural considerations and conclusions from this study are also applicable to other ionic conductors like $Li_{1+x}Al_xTi_{2-x}P_3O_{12}$ [18].

3. Structure and conduction pathway

The NASICON structure consists of a three-dimensional framework of corner-sharing MO_6 octahedra and PO_4 tetrahedra. Depending on the composition, the crystal structure can either be rhombohedral, monoclinic or triclinic (as the low-temperature phase of $LiZr_2(PO_4)_3$ [19] or $LiSn_2(PO_4)_3$ [20] which will not be further considered in this survey).

The first reported NASICON, $Na_{1+x}Zr_2Si_xP_{3-x}O_{12}$ ($0 \le x \le 3$), has a rhombohedral structure ($R\bar{3}c$) except for $1.8 \le x \le 2.2$. In this interval, the material undergoes a monoclinic distortion (C2/c), see Fig. 1.

In the rhombohedral NASICON structure, the Na^+ ions occupy two different sites when $x > 0$. The Na(1) sites are sixfold coordinated to the oxygen ions of three $(Si,P)O_4$ tetrahedra above and below (coordinate (0,0,0)), the Na(2) sites are also sixfold coordinated to oxygen ions of three coplanar $(Si,P)O_4$ tetrahedra (coordinate (*x*,*y*,0.25)). This site occupancy was also confirmed very recently for Li^+ ions in $Li_{1+x}Al_xTi_{2-x}P_3O_{12}$ [21]. For NASICON materials with only one Na per formula unit, only the Na(1) position is occupied. For monoclinic NASICON materials, there is a third sodium position. The Na(3) sites are threefold coordinated to the oxygen ions of three ZrO_6 octahedra. The conduction occurs by jumping from the Na(1) to the Na(2) or Na(3) sites, which represent a distance of approximately 3 Å depending on the composition of the material. The Na^+ ions jump from one position to the next through oxygen triangles T1 and T2, the bottlenecks for the Na^+ conduction, shown in Fig. 2 in the rhombohedral structure of $Na_3M_2^{III}(PO_4)_3$ (data with M^{III} = Sc [22]).

4. Ionic conductivity

4.1. Range of ionic conductivity of NASICON materials

Depending on the composition, the ionic conductivity of a material with a NASICON structure can vary by several orders of magnitude. As a reference, and because it is still one of the best values achieved to date, the conductivity of $Na_3Zr_2Si_2PO_{12}$ is $6.7 \cdot 10^{-4}$ S cm^{-1} at room temperature and 0.2 S cm^{-1} at 300 °C [9]. To compete with a liquid electrolyte, the ionic conductivity of a solid electrolyte should be about 10^{-2} S cm^{-1} at room temperature [23].

In this literature study, more than 150 different materials were found with the general formula $Na_{1+2w+x-y+z}M_w^{(II)}M_x^{(III)}M_y^{(V)}M_{2-w-x-y}^{(IV)}(SiO_4)_z(PO_4)_{3-z}$ containing different cations $M^{(II)}$, $M^{(III)}$, $M^{(IV)}$ and $M^{(V)}$ and different values of *w*, *x*, *y* and *z*. The conductivities at 300 °C and at room temperature that have been measured to date for more than 110 of these materials are summarized in Table 1–4. Some conductivity values have been extrapolated down to room temperature with help of the activation energy found in the literature and the Arrhenius law (the value of the pre-exponential factor of the Arrhenius law, A, is also listed in Table 1–4). Those NASICON materials for which the activation energy has not been calculated are not included in these tables because their conductivity at room temperature could not be extrapolated. For those NASICON materials which show a phase transition, the activation energy differed at low temperature (LT) and high temperature (HT). Typically, the transition from the low-temperature phase to the high-temperature phase occurs around 400 °C + 200 °C and depends on the composition.

Although the microstructure and particularly the porosity have a significant impact on the conductivity, this influence on the data could not be considered because in most of the papers this information was missing. Overall, it appears that the general trends

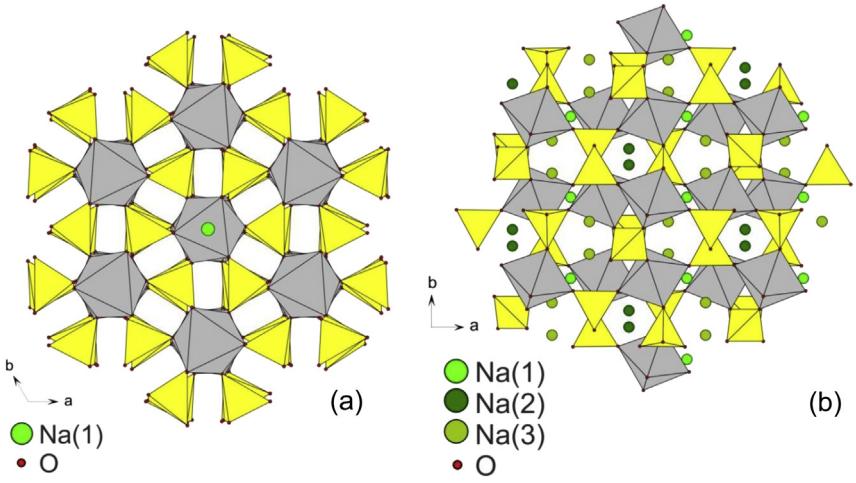

Fig. 1. The projection in the $a-b$ plane of (a) the rhombohedral $R\bar{3}c$ structure of $NaZr_2(PO_4)_3$ and (b) the monoclinic C2/c structure of $Na_3Zr_2(SiO_4)_2(PO_4)$ [9]. The yellow tetrahedra and the grey octahedra correspond to $(Si,P)O_4$ and ZrO_6 units, respectively.

were identified and the missing correction for porosity is leading to a larger scatter of the compiled data.

4.2. Correlation between ionic conductivity and composition

In order to find a correlation between the conductivity of sodium ions and their compositions, an effective mean ionic radius of the cations $M^{(II)}$, $M^{(III)}$, $M^{(IV)}$ and $M^{(V)}$, r_{eff}, was defined as a geometrical parameter. For the general formula $Na_{1+2w+x-y+z}M^{(II)}_wM^{(III)}_xM^{(V)}_yM^{(IV)}_{2-w-x-y}(SiO_4)_z(PO_4)_{3-z}$, r_{eff} was calculated using the equation:

$$r_{eff} = (r_{M^{(II)}}w + r_{M^{(III)}}x + r_{M^{(V)}}y + r_{M^{(IV)}}(2-w-x-y))/2 \qquad (1)$$

In this equation, all ionic radii were taken from Ref. [24]. Fig. 3a illustrates the evolution of the conductivity at room temperature as a function of the amount of sodium per formula unit, whereas Fig. 3b shows the evolution of the conductivity at room temperature as a function of r_{eff}.

In Fig. 3a the largest scatter of conductivity appears for compositions with one Na per formula unit, i.e. $NaM^{(IV)}_2(PO_4)_3$. Since the conductivity changes by about 10 orders of magnitude, this can be interpreted on the one hand as a significant impact of the $M^{(IV)}$ cations influencing the bond strength and local coordination sphere of the sodium ions. However, on the other hand it also can be interpreted as experimental uncertainty of the sodium content, because a very small change of charge carriers can cause a huge variation in conductivity. With higher sodium concentrations this scatter is reduced and a clear trend is visible towards higher conductivity.

The dependence of the ionic conductivity on r_{eff} is also associated with a large scatter of the data points. Nevertheless, a maximum in conductivity is observed at about 0.72 Å and a lot of

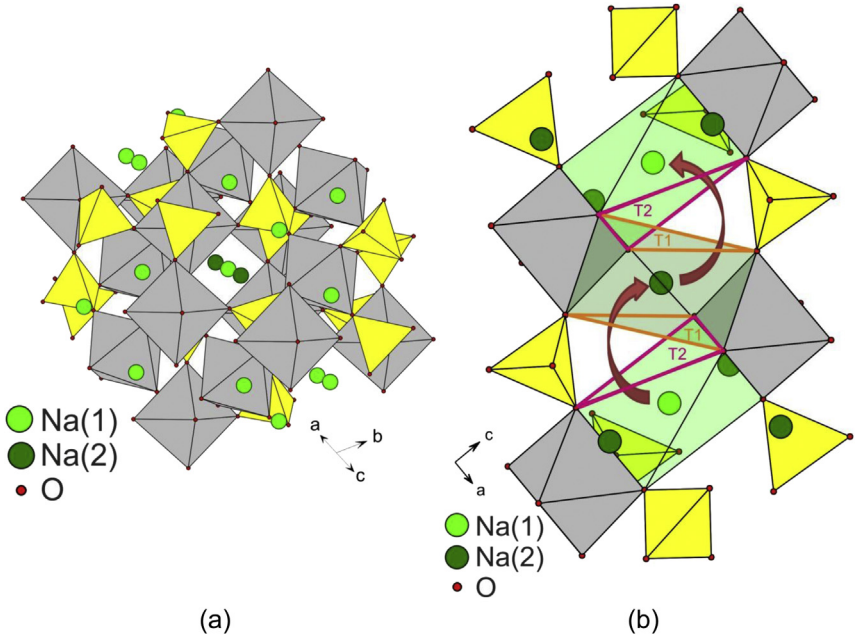

Fig. 2. Representation of the conduction pathway in the NASICON structure. As an example the crystallographic data of $Na_3Sc_2(PO_4)_3$ [21] were chosen. (a) highlights one conduction channel along (2 −1 4) and (b) represents the Na^+ jumps from the Na(1) to the Na(2) site and illustrates the bottlenecks T1 and T2. The yellow tetrahedra and the grey octahedra correspond to PO_4 and $M^{III}O_6$ units, respectively.

Table 1
Conductivity at room temperature and 300 °C, activation energy and pre-exponential factor of compositions with the formula $Na_{1+y}M_x^{(IV)}M'^{(IV)}_{2-x}(SiO_4)_y(PO_4)_{3-y}$. The values with an asterisk were calculated using the Arrhenius equation (Eq. (2)).

NASICON material	σ_{RT} [S cm^{-1}]	$\sigma_{300\,°C}$ [S cm^{-1}]	E_a [eV]	A [S K cm^{-1}]	Ref.
$NaZr_2(PO_4)_3$	4.50E-06	4.89E-05*	0.47	1.18E+05*	[9,25,37]
$NaGe_2(PO_4)_3$	1.10E-12*	2.56E-06*	0.81	1.61E+04*	[26]
$NaTi_2(PO_4)_3$	4.43E-10*	2.98E-05*	0.62	3.99E+03*	[26,37,38]
$NaHf_2(PO_4)_3$	8.77E-10*	1.03E-04*	0.65	2.54E+04*	[26,32,38]
$NaSn_2(PO_4)_3$	4.65E-09*	1.50E-05*	0.47	1.22E+02*	[25,39]
$NaGe_{0.5}Ti_{1.5}(PO_4)_3$	5.91E-13*	8.70E-07*	0.798	5.43E+03*	[25,29]
$NaGeTi(PO_4)_3$	8.50E-12*	2.01E-06*	0.7	1.72E+03*	[25,29]
$NaGe_{1.5}Ti_{0.5}(PO_4)_3$	3.13E-11*	8.90E-06*	0.71	9.36E+03*	[25,29]
$NaSn_{0.5}Ti_{1.5}(PO_4)_3$	1.77E-11*	1.29E-06*	0.637	3.09E+02*	[25,40]
$NaSnTi(PO_4)_3$	6.86E-11*	3.64E-06*	0.62	6.18E+02*	[25,40]
$NaSn_{1.5}Ti_{0.5}(PO_4)_3$	5.14E-10*	6.11E-06*	0.54	2.06E+02*	[25,40]
$NaSn_{0.5}Zr_{1.5}(PO_4)_3$	4.23E-11*	2.70E-06*	0.63	5.62E+02*	[25,39]
$NaSnZr(PO_4)_3$	2.47E-10*	1.58E-05*	0.63	3.28E+03*	[25,39]
$NaSn_{1.5}Zr_{0.5}(PO_4)_3$	7.91E-10*	2.40E-05*	0.59	2.22E+03*	[25,39]
$NaNbZr(PO_4)_3$	2.49E-08*	3.10E-04	0.54	9.97E+03*	[28]
$NaNbTi(PO_4)_3$	1.59E-06*	1.00E-03	0.38	1.26E+03*	[28]
$NaMoZr(PO_4)_3$	2.06E-09*	3.10E-05	0.55	1.22E+03*	[28]
$NaMoTi(PO_4)_3$	3.07E-07*	2.80E-04	0.4	5.28E+02*	[28]
$Na_3Zr_2(SiO_4)_2(PO_4)$	6.70E-04	2.00E-01	0.33 (LT)/0.27 (HT)	7.56E+04*	[9,16,41]
$Na_4Zr_2(SiO_4)_3$	8.87E-09	1.10E-03	0.38	7.01E+00*	[42,43]
$Na_{2.4}Hf_2(SiO_4)_{1.4}(PO_4)_{1.6}$	7.30E-04	1.27E-01*	0.4 (LT)/0.28 (HT)	2.11E+04*	[32]
$Na_{2.5}Hf_2(SiO_4)_{1.5}(PO_4)_{1.5}$	1.87E-04	1.34E-02	0.27	2.04E+03*	[32]
$Na_{2.6}Hf_2(SiO_4)_{1.6}(PO_4)_{1.4}$	5.90E-04	1.42E-1*	0.35 (LT)/0.26 (HT)	1.54E+04*	[32]
$Na_{2.8}Hf_2(SiO_4)_{1.8}(PO_4)_{1.2}$	6.90E-04	1.57E-1*	0.42 (LT)/0.23 (HT)	9.46E+03*	[32]
$Na_3Hf_2(SiO_4)_2(PO_4)$	1.10E-03	1.51E-1*	0.35 (LT)/0.21 (HT)	6.07E+03*	[32]
$Na_{3.2}Hf_2(SiO_4)_{2.2}(PO_4)_{0.8}$	2.30E-03	2.24E-1*	0.36 (LT)/0.19 (HT)	6.02E+03*	[32]
$Na_{3.4}Hf_2(SiO_4)_{2.4}(PO_4)_{0.6}$	1.40E-03	7.68E-2*	0.35 (LT)/0.22 (HT)	3.79E+03*	[32]
$Na_{3.6}Hf_2(SiO_4)_{2.6}(PO_4)_{0.4}$	1.20E-03	5.76E-2*	0.34 (LT)/0.29 (HT)	1.17E+04*	[32]
$Na_{3.8}Hf_2(SiO_4)_{2.8}(PO_4)_{0.2}$	3.20E-04	4.31E-2*	0.35 (LT)/0.27 (HT)	5.85E+03*	[32]
$Na_{3.5}Hf_{0.2}Ti_{1.8}(SiO_4)_{1.5}(PO_4)_{1.5}$	3.36E-04	3.52E-02	0.245	1.39E+03*	[44]
$Na_{3.5}Hf_{0.6}Ti_{1.4}(SiO_4)_{1.5}(PO_4)_{1.5}$	2.81E-04	3.61E-02	0.27	3.07E+03*	[44]
$Na_{3.5}HfTi(SiO_4)_{1.5}(PO_4)_{1.5}$	1.35E-04	3.47E-02	0.26	9.99E+02*	[44]
$Na_{3.5}Hf_{1.4}Ti_{0.6}(SiO_4)_{1.5}(PO_4)_{1.5}$	8.70E-05	1.19E-02	0.5	7.34E+06*	[44]
$Na_3Hf_{0.2}Ti_{1.8}(SiO_4)_2(PO_4)$	2.32E-04	1.33E-02	0.3	8.15E+03*	[44]
$Na_3Hf_{0.4}Ti_{1.6}(SiO_4)_2(PO_4)$	9.60E-05	8.40E-03	0.31	4.97E+03*	[44]
$Na_3Hf_{0.6}Ti_{1.4}(SiO_4)_2(PO_4)$	2.84E-04	1.48E-02	0.29	6.76E+03*	[44]
$Na_3Hf_{0.8}Ti_{1.2}(SiO_4)_2(PO_4)$	1.78E-04	7.00E-03	0.31	9.22E+03*	[44]
$Na_3HfTi(SiO_4)_2(PO_4)$	1.31E-04	6.50E-03	0.28	2.11E+03*	[44]
$Na_3Ti_{0.1}Zr_{1.9}(SiO_4)_2(PO_4)$	1.10E-04*	6.90E-02	0.38 (LT)/0.2 (HT)	8.69E+04*	[45]
$Na_3Ti_{0.2}Zr_{1.8}(SiO_4)_2(PO_4)$	8.75E-05*	5.50E-02	0.38 (LT)/0.2 (HT)	6.91E+04*	[45]
$Na_3Ti_{0.3}Zr_{1.7}(SiO_4)_2(PO_4)$	9.87E-05*	6.20E-02	0.38 (LT)/0.2 (HT)	7.80E+04*	[45]

compositions have been investigated in this region. Considering a deviation of only 0.05 Å from this ideal r_{eff}, the ionic conductivity drops by one order of magnitude. Besides the sensitivity of the ionic conductivity on r_{eff}, the number of charge carriers has to be considered. In Fig. 3b the sodium content is grouped in three classes of which the compositions with 2.5 ≤ Na/mol ≤ 3.5 show the highest conductivity values as already presented in Fig. 3a.

Indeed, both the Na concentration and the size of the M cations determine the properties of a NASICON material and only when both parameters are simultaneously at the optimum value, the

Table 2
Conductivity at room temperature and 300 °C, activation energy and pre-exponential factor of compositions with the formula $Na_{1+2x+y}M_x^{(II)}M'^{(IV)}_{2-x}(SiO_4)_y(PO_4)_{3-y}$. The values with an asterisk were calculated using the Arrhenius equation (Eq. (2)).

NASICON material	σ_{RT} [S cm^{-1}]	$\sigma_{300\,°C}$ [S cm^{-1}]	E_a [eV]	A [S K cm^{-1}]	Ref.
$Na_{3.08}Mg_{0.04}Zr_{1.96}(SiO_4)_2(PO_4)$	3.70E-04*	1.60E-01	0.36 (LT)/0.19(HT)	1.34E+05*	[45]
$Na_{3.2}Mg_{0.1}Zr_{1.9}(SiO_4)_2(PO_4)$	2.08E-04*	6.20E-02	0.34 (LT)/0.22(HT)	3.46E+04*	[45]
$Na_{3.6}Mg_{0.3}Zr_{1.7}(SiO_4)_2(PO_4)$	9.02E-05*	3.90E-02	0.36 (LT)/0.25(HT)	3.27E+04*	[45]
$Na_{3.08}Zn_{0.04}Zr_{1.96}(SiO_4)_2(PO_4)$	2.19E-05*	3.50E-02	0.43 (LT)/0.31(HT)	1.21E+05*	[45]
$Na_{3.2}Zn_{0.1}Zr_{1.9}(SiO_4)_2(PO_4)$	8.44E-05*	4.40E-02	0.37 (LT)/0.31(HT)	4.52E+04*	[45]
$Na_{3.4}Zn_{0.2}Zr_{1.4}(SiO_4)_2(PO_4)$	5.05E-04*	4.90E-02	0.28(LT)/0.14(HT)	8.14E+03*	[45]
$Na_{3.6}Zn_{0.3}Zr_{1.7}(SiO_4)_2(PO_4)$	1.75E-05*	2.80E-02	0.43 (LT)/0.31(HT)	9.68E+04*	[45]
$Na_{3.28}Mg_{0.04}Zr_{1.96}(SiO_4)_{2.2}(PO_4)_{0.8}$	8.06E-04*	2.40E-01	0.34 (LT)/0.19(HT)	1.34E+05*	[46]
$Na_{3.36}Mg_{0.08}Zr_{1.92}(SiO_4)_{2.2}(PO_4)_{0.8}$	4.64E-04*	9.50E-02	0.32 (LT)/0.19(HT)	3.55E+04*	[46]
$Na_{3.52}Mg_{0.16}Zr_{1.84}(SiO_4)_{2.2}(PO_4)_{0.8}$	1.71E-04*	2.00E-02	0.29 (LT)/0.19(HT)	4.07E+03*	[46]
$Na_{3.36}Zn_{0.08}Zr_{1.92}(SiO_4)_{2.2}(PO_4)_{0.8}$	1.10E-03*	2.10E-01	0.32 (LT)/0.17(HT)	7.20E+04*	[47]
$Na_{3.36}Cu_{0.08}Zr_{1.92}(SiO_4)_{2.2}(PO_4)_{0.8}$	5.31E-04*	2.09E-01	0.36 (LT)/0.17(HT)	1.59E+05*	[47]
$Na_{3.36}Co_{0.08}Zr_{1.92}(SiO_4)_{2.2}(PO_4)_{0.8}$	1.03E-03*	2.40E-01	0.33 (LT)/0.18(HT)	1.03E+05*	[47]
$Na_{3.232}Co_{0.016}Zr_{1.984}(SiO_4)_{2.2}(PO_4)_{0.8}$	1.41E-03*	2.40E-01	0.31 (LT)/0.19(HT)	7.31E+04*	[46]
$Na_{3.52}Co_{0.16}Zr_{1.84}(SiO_4)_{2.2}(PO_4)_{0.8}$	5.88E-04*	1.00E-01	0.31 (LT)/0.22(HT)	3.05E+04*	[46]

Table 3
Conductivity at room temperature and 300 °C, activation energy and pre-exponential factor of compositions with the formula $Na_{1+x+y}M_x^{(III)}M'^{(IV)}_{2-x}(SiO_4)_y(PO_4)_{3-y}$. The values with an asterisk were calculated using the Arrhenius equation (Eq. (2)).

NASICON material	σ_{RT} [S cm^{-1}]	$\sigma_{300\ °C}$ [S cm^{-1}]	E_a [eV]	A [S K cm^{-1}]	Ref.
$Na_{1.2}In_{0.2}Zr_{1.8}(PO_4)_3$	2.08E-07*	1.46E-03*	0.49	1.19E+04*	[36]
$Na_{1.4}In_{0.4}Zr_{1.6}(PO_4)_3$	9.76E-07*	3.25E-03*	0.45	1.18E+04*	[36]
$Na_{1.5}Al_{0.5}Zr_{1.5}(PO_4)_3$	5.70E-06	6.70E-04	0.54	2.28E+06*	[48]
$Na_{1.5}Cr_{0.5}Zr_{1.5}(PO_4)_3$	1.00E-05	5.50E-04	0.425	4.55E+04*	[48,49]
$Na_{1.5}Ga_{0.5}Zr_{1.5}(PO_4)_3$	3.40E-06	3.40E-04	0.518	5.78E+05*	[48]
$Na_{1.5}In_{0.5}Zr_{1.5}(PO_4)_3$	2.90E-05	1.90E-03	0.477	1.00E+06*	[48,49,50]
$Na_{1.5}Sc_{0.5}Zr_{1.5}(PO_4)_3$	5.80E-05	2.30E-03	0.425	2.64E+05*	[48]
$Na_{1.5}Y_{0.5}Zr_{1.5}(PO_4)_3$	5.60E-05	1.40E-03	0.378	4.09E+04*	[48,51]
$Na_{1.5}Yb_{0.5}Zr_{1.5}(PO_4)_3$	3.00E-05	1.20E-03	0.425	1.37E+05*	[48,49,52]
$Na_2AlZr(PO_4)_3$	1.20E-06	2.30E-04	0.586	2.88E+06*	[48]
$Na_2CrZr(PO_4)_3$	2.50E-05	8.50E-04	0.409	6.11E+04*	[48]
$Na_{2.2}In_{1.2}Zr_{0.8}(PO_4)_3$	2.63E-06*	4.99E-03*	0.42	9.86E+03*	[36]
$Na_{2.3}Yb_{1.3}Zr_{0.7}(PO_4)_3$	6.03E-06*	5.50E-03	0.4	1.04E+04*	[48,49]
$Na_{2.5}Cr_{1.5}Zr_{0.5}(PO_4)_3$	1.80E-04	7.20E-03	0.425	8.20E+05*	[48]
$Na_{2.5}In_{1.5}Zr_{0.5}(PO_4)_3$	1.00E-04	6.40E-03	0.472	2.84E+06*	[36,48]
$Na_{2.5}Sc_{1.5}Zr_{0.5}(PO_4)_3$	5.60E-04	1.20E-02	0.357	1.81E+05*	[48]
$Na_{2.5}Y_{1.5}Zr_{0.5}(PO_4)_3$	4.60E-05	2.50E-03	0.456	7.00E+05*	[48,51]
$Na_{2.5}Yb_{1.5}Zr_{0.5}(PO_4)_3$	1.90E-04	2.40E-02	0.544	8.89E+07*	[48,49,52]
$Na_{2.5}Er_{1.5}Zr_{0.5}(PO_4)_3$	1.24E-09*	1.00E-04	0.64	2.43E+04*	[52,53]
$Na_{2.5}Dy_{1.5}Zr_{0.5}(PO_4)_3$	1.65E-08*	6.30E-04	0.6	6.82E+04*	[53]
$Na_{2.6}In_{1.6}Zr_{0.4}(PO_4)_3$	2.81E-06*	1.13E-02*	0.46	5.00E+04*	[36]
$Na_{2.8}In_{1.8}Zr_{0.2}(PO_4)_3$	2.38E-06*	5.45E-03*	0.43	1.32E+04*	[36]
$Na_{2.85}In_{1.85}Zr_{0.15}(PO_4)_3$	5.25E-07*	3.10E-03	0.5	4.43E+04*	[49]
$Na_{2.95}Cr_{1.95}Zr_{0.05}(PO_4)_3$	4.22E-06*	9.80E-03	0.45	5.09E+04*	[49]
$Na_3Cr_2(PO_4)_3$	1.70E-07	7.00E-03	0.68 (LT)/0.38 (HT)	1.58E+07*	[48,49,54]
$Na_3Fe_2(PO_4)_3$	1.20E-07	9.00E-03	0.82 (LT)/0.41 (HT)	2.60E+09*	[48,54]
$Na_3In_2(PO_4)_3$	1.76E-07*	9.00E-04	0.4923	1.10E+04*	[36,48]
$Na_3Sc_2(PO_4)_3$	2.27E-05*	5.68E-02*	0.352	6.03E+03*	[48,55]
$Na_{1.4}Al_{0.4}Ge_{1.6}(PO_4)_3$	7.28E-10*	6.98E-05*	0.63	9.68E+03*	[56,57]
$Na_{1.4}Al_{0.4}Sn_{1.6}(PO_4)_3$	1.41E-08*	4.42E-04*	0.57	1.81E+04*	[56,57]
$Na_{1.4}Al_{0.4}Ti_{1.6}(PO_4)_3$	5.60E-08	1.43E-03*	0.52	1.03E+04*	[56,57]
$Na_{1.6}Al_{0.6}Ti_{1.4}(PO_4)_3$	1.10E-07	2.57E-03*	0.56	9.59E+04*	[56,57]
$Na_{1.8}Al_{0.8}Ti_{1.2}(PO_4)_3$	1.20E-07	2.74E-03*	0.55	7.09E+04*	[56,57]
$Na_{1.9}Al_{0.9}Ti_{1.1}(PO_4)_3$	1.30E-07	1.82E-03*	0.51	1.62E+04*	[56,57]
$Na_{1.4}In_{0.4}Ti_{1.6}(PO_4)_3$	1.86E-08*	3.03E-04*	0.535	6.13E+03*	[27]
$Na_{1.4}In_{0.4}Sn_{1.6}(PO_4)_3$	2.72E-08*	4.04E-04*	0.53	7.38E+03*	[27]
$Na_{1.4}In_{0.4}Hf_{1.6}(PO_4)_3$	1.86E-07*	2.67E-04*	0.405	3.89E+02*	[27]
$Na_{2.04}Y_{0.04}Zr_{1.96}(SiO_4)_2(PO_4)$	2.08E-04*	6.20E-02	0.34 (LT)/0.22 (HT)	3.46E+04*	[45]
$Na_{2.1}Y_{0.1}Zr_{1.9}(SiO_4)_2(PO_4)$	1.98E-03*	1.10E-01	0.25 (LT)/0.16 (HT)	9.93E+03*	[45]
$Na_{2.3}Y_{0.3}Zr_{1.7}(SiO_4)_2(PO_4)$	9.76E-05*	2.00E-02	0.32 (LT)/0.30 (HT)	7.46E+03*	[45]
$Na_{2.5}Sc_{0.2}Zr_{1.8}(SiO_4)_{1.3}(PO_4)_{1.7}$	3.19E-04*	4.50E-02	0.3	1.12E+04*	[58]
$Na_3Sc_{1.5}Zr_{0.5}(SiO_4)_{0.5}(PO_4)_{2.5}$	1.17E-04*	2.90E-02	0.33	1.32E+04*	[58]
$Na_3ScZr(SiO_4)_2(PO_4)$	1.82E-04*	3.10E-02	0.31	9.43E+03*	[58]
$Na_3Sc_{0.8}Zr_{1.2}(SiO_4)_{1.2}(PO_4)_{1.8}$	1.42E-04*	2.90E-02	0.32	1.09E+04*	[58]
$Na_3Sc_{0.5}Zr_{1.5}(SiO_4)_{1.5}(PO_4)_{1.5}$	1.41E-04*	1.07E-01	0.30 (LT)/0.23 (HT)	6.45E+03*	[58]
$Na_3Sc_{0.2}Zr_{1.8}(SiO_4)_{1.8}(PO_4)_{1.2}$	1.90E-04*	1.20E-01	0.37 (LT)/0.21 (HT)	4.83E+03*	[58]
$Na_{3.3}Sc_{0.3}Zr_{1.7}(SiO_4)_2(PO_4)$	4.14E-04*	1.79E-01	0.37 (LT)/0.20 (HT)	5.89E+03*	[58]
$Na_{3.5}Sc_{0.5}Zr_{1.5}(SiO_4)_2(PO_4)$	4.88E-04*	1.00E-01	0.32	3.73E+04*	[58]
$Na_{2.7}Sc_{0.2}Zr_{1.8}(SiO_4)_{1.5}(PO_4)_{1.5}$	8.87E-05*	8.10E-02	0.4	1.53E+05*	[58]

conductivity will be high. Therefore two main results can be derived from Fig. 3:

- For values of r_{eff} far from 0.72 ± 0.1 Å (i.e. the ionic radius of Zr [24]), the ionic conductivity decreases exponentially.

Table 4
Conductivity at room temperature and 300 °C, activation energy and pre-exponential factor of compositions with the formula $Na_{1-x+y}M_x^{(V)}M'^{(IV)}_{2-x}(SiO_4)_y(PO_4)_{3-y}$. The values with an asterisk were calculated using the Arrhenius equation (Eq. (2)).

NASICON material	σ_{RT} [S cm^{-1}]	$\sigma_{300\ °C}$ [S cm^{-1}]	E_a [eV]	A [S K cm^{-1}]	Ref.
$Na_{2.96}Nb_{0.04}Zr_{1.96}(SiO_4)_2(PO_4)$	4.95E-03*	1.30E-01	0.21	5.23E+03*	[45]
$Na_{2.9}Nb_{0.1}Zr_{1.9}(SiO_4)_2(PO_4)$	1.87E-03*	4.90E-02	0.21	1.98E+03*	[45]
$Na_{2.96}Ta_{0.04}Zr_{1.96}(SiO_4)_2(PO_4)$	9.40E-04*	1.10E-01	0.17	2.09E+02*	[45]
$Na_{2.9}Ta_{0.1}Zr_{1.9}(SiO_4)_2(PO_4)$	5.30E-04*	6.20E-02	0.17	1.18E+02*	[45]
$Na_{2.96}V_{0.04}Zr_{1.96}(SiO_4)_2(PO_4)$	1.20E-03*	1.40E-01	0.21	1.27E+03*	[45]
$Na_{2.9}V_{0.1}Zr_{1.9}(SiO_4)_2(PO_4)$	4.78E-04*	9.80E-02	0.32	3.66E+04*	[45]

- As the number of charge carriers increases, so too does the conductivity, until a maximum concentration is reached, corresponding either to the half-filled occupancy of the Na sites or a structural change resulting in a steric barrier. In general, compositions with ≥2.5 mol sodium per formula unit show a high ionic conductivity between $2\cdot10^{-5}$ and $8\cdot10^{-3}$ S cm^{-1}.

As r_{eff} is an arithmetic average, it is important to look at the difference in ionic radii between the M cations in the same compound. It might be expected that compositions with cations of a similar size have a higher conductivity than those which contain cations of very different sizes due to the different Coulombic and steric interactions along the conduction pathway. Fig. 4 shows the conductivity at room temperature as a function of the difference between the ionic radii of M and M′ ($\Delta r_{M-M'}$) in $Na_{1+2w+x-y+z}M_w^{(II)}M_x^{(III)}M_y^{(V)}M^{(IV)}_{2-w-x-y}(SiO_4)_z(PO_4)_{3-z}$. No particular dependence is evident, indicating that the difference between

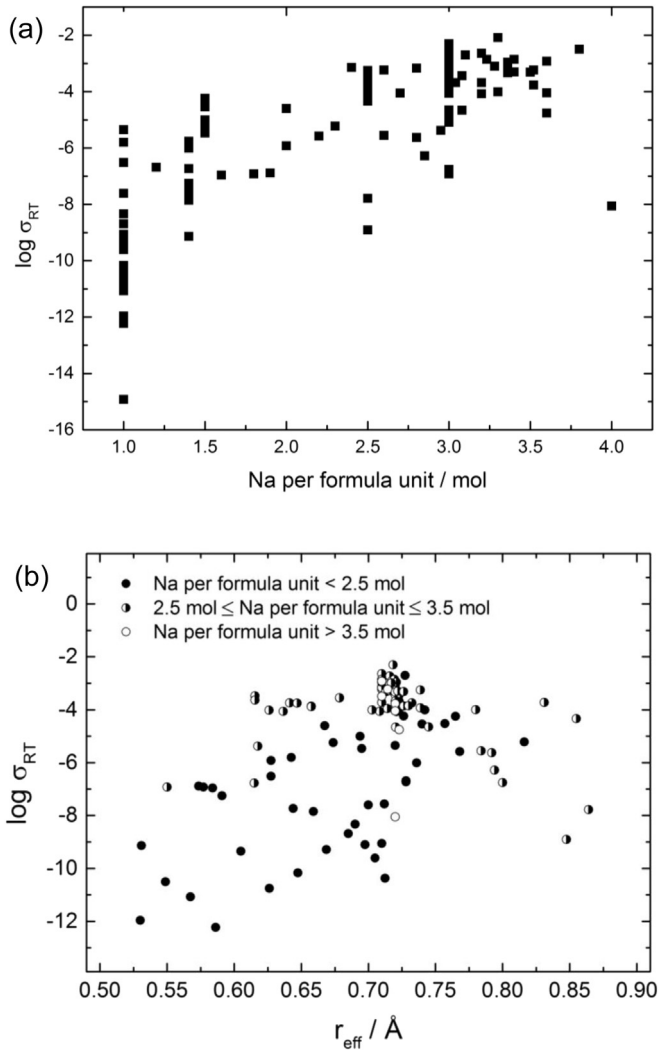

Fig. 3. Conductivity at room temperature, σ_{RT}, as a function of the Na^+ concentration (a) and the effective ionic radius of the M cations (b) in $Na_{1+2w+x-y+z}M_w^{(II)}M_x^{(III)}M_y^{(V)}M_{2-w-x-y}^{(IV)}(SiO_4)_z(PO_4)_{3-z}$. In (b) different amounts of Na per formula unit are distinguished (filled symbols represent materials with less than 2.5 mol Na per formula unit, open symbols more than 3.5 mol Na per formula unit and half-filled symbols the compositions in between).

the ionic radii of the M cations is not important, and only the arithmetic average of their ionic radii must be close to 0.72 Å.

Two examples shown in Fig. 4 are $NaGe_2(PO_4)_3$ and $NaSnTi(PO_4)_3$. Both materials have very similar conductivities at room temperature ($1.1\cdot10^{-12}$ S cm^{-1} [25] and $6.9\cdot10^{-11}$ S cm^{-1} [26], respectively), although in the first case M = M′ = Ge, and in the second case M = Sn, M′ = Ti with $\Delta r_{Sn-Ti} = 0.085$ Å.

Two further examples are $Na_{1.4}In_{0.4}Ti_{1.6}(PO_4)_3$ with a conductivity at room temperature of $1.9\cdot10^{-8}$ S cm^{-1} and $Na_{1.4}In_{0.4}Sn_{1.6}(PO_4)_3$ with a conductivity of $2.7\cdot10^{-8}$ S cm^{-1} [27]. The sodium content is the same in both cases, as is the conductivity. However, the differences between M and M′ for the two compounds are different ($\Delta r_{In-Ti} = 0.195$ Å, $\Delta r_{In-Sn} = 0.11$ Å).

For equal $\Delta r_{M-M'}$, like in the case of $NaNbTi(PO_4)_3$ ($\Delta r_{Nb-Ti} = 0.075$ Å) and $NaGe_{0.5}Ti_{1.5}(PO_4)_3$ (($\Delta r_{Ge-Ti} = 0.075$ Å), different conductivity can also be observed ($1.6\cdot10^{-6}$ S cm^{-1} [28] and $5.9\cdot10^{-13}$ S cm^{-1} [25,29], respectively), which validates the importance of the arithmetic average of the ionic radii of the M cations ($r_{eff} = 0.64$ Å and $r_{eff} = 0.59$ Å for $NaNbTi(PO_4)_3$ and $NaGe_{0.5}Ti_{1.5}(PO_4)_3$, respectively) but not their difference.

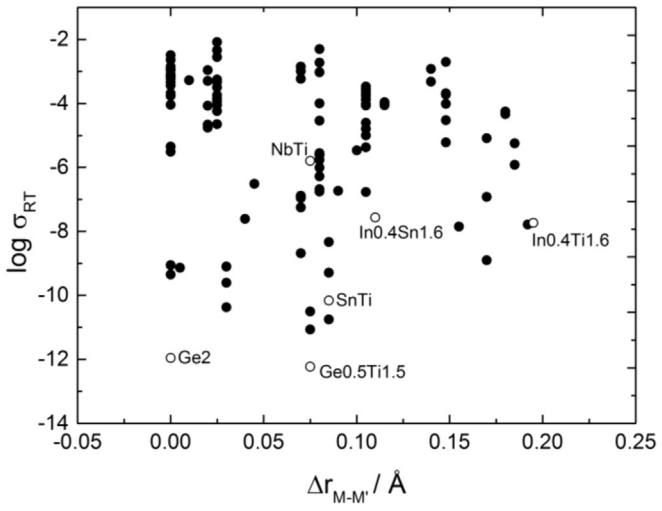

Fig. 4. Influence of the difference of ionic radius between M and M′ ($\Delta r_{M-M'}$) on the conductivity of $Na_{1+2x+y+z}M_x^{(II)}M_y^{(III)}M_{2-x-y}^{(IV)}(SiO_4)_z(PO_4)_{3-z}$. Selected data points refer to $NaGe_2(PO_4)_3$ (Ge_2), $NaSnTi(PO_4)_3$ (SnTi), $Na_{1.4}In_{0.4}Ti_{1.6}(PO_4)_3$ ($In_{0.4}Ti_{1.6}$), $Na_{1.4}In_{0.4}Sn_{1.6}(PO_4)_3$ ($In_{0.4}Sn_{1.6}$), $NaGe_{0.5}Ti_{1.5}(PO_4)_3$ ($Ge_{0.5}Ti_{1.5}$) and $NaNbTi(PO_4)_3$ (NbTi).

4.3. Factors influencing the ionic conductivity

4.3.1. Activation energy and pre-exponential factor

The ionic conductivity follows the Arrhenius law:

$$\sigma T = Ae^{\frac{-E_a}{RT}} \quad (2)$$

where σ is the ionic conductivity, T is the absolute temperature, E_a is the activation energy composed of a barrier energy ΔH_b for charge migration and a relaxation energy ΔH_r of the local lattice environment, A is a pre-exponential constant containing the number of charge carriers, jump distance and attempt frequency [30,31], and R is the gas constant.

As the pre-exponential factor A includes the number of charge carriers, this validates the observation that the conductivity increases with the number of charge carriers (Fig. 3a). The smaller increase at high sodium concentrations is probably related to the reduced attempt frequency, because the attempts for successful

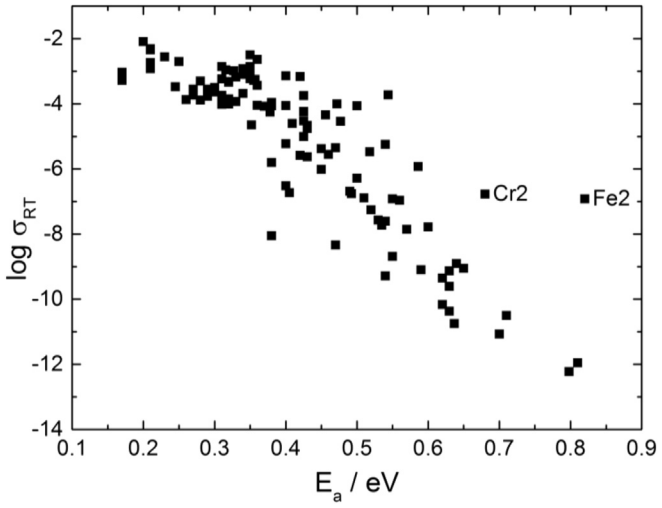

Fig. 5. Impact of E_a on the conductivity at room temperature. The two data points labelled Cr_2 and Fe_2 correspond to $Na_3Cr_2(PO_4)_3$ and $Na_3Fe_2(PO_4)_3$, respectively.

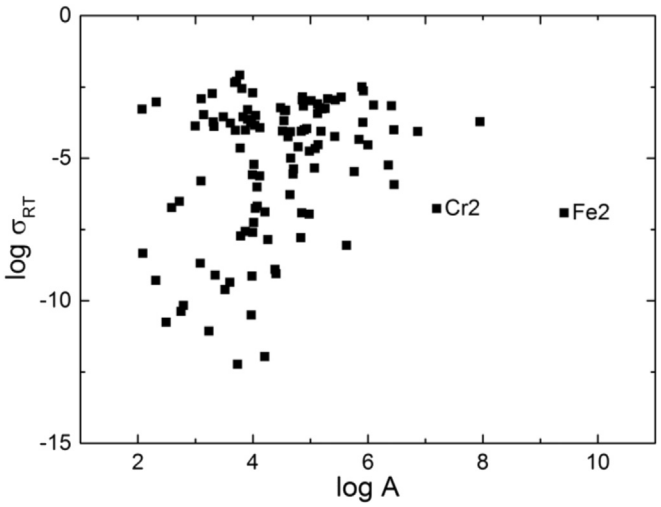

Fig. 6. Impact of A on the conductivity at room temperature. The two data points labelled Cr_2 and Fe_2 correspond to $Na_3Cr_2(PO_4)_3$ and $Na_3Fe_2(PO_4)_3$, respectively.

jump to the next neighbouring site are more and more blocked by another Na ion.

The influence of the activation energy and the pre-exponential factor on the conductivity is depicted in Figs. 5 and 6, respectively.

In Fig. 5, a clear trend is observed in which the ionic conductivity decreases with increasing activation energy. Ge- and Ti-based NASICONs have the highest activation energy and lowest conductivity, whereas Ta-, V-, Zr-, Sc- and Hf-based NASICONs with >1.5 mol Si per formula unit have the lowest activation energy and highest conductivity. This highlights the importance of substituting P with Si. As an example, the evolution of the activation energies and conductivities at room temperature as a function of x in the solid solution $Na_{1+x}Hf_2Si_xP_{3-x}O_{12}$ [32] is summarized in Fig. 7. This particular example corroborates the conclusion drawn in our analysis: the substitution of P with Si assures an increase of the conductivity until a maximum is reached depending on the M cations involved (in this case $x = 2.2$).

The dependence of the ionic conductivity on the pre-exponential factor is less evident. Although the conductivity increases with an increasing pre-exponential factor, there is a large scatter, particularly for those compositions with high ionic conductivity. Therefore, the activation energy has a much stronger impact on the conductivity than the number of charge carriers.

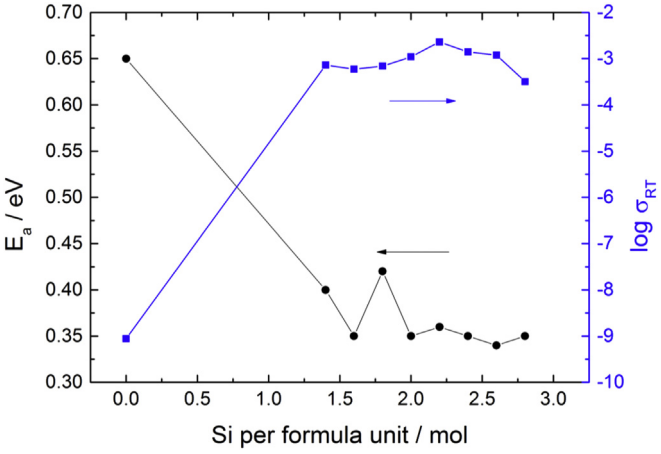

Fig. 7. Impact of the amount of Si per formula unit on the activation energy and conductivity at room temperature in $Na_{1+x}Hf_2Si_xP_{3-x}O_{12}$ as reported in Ref. [32].

The NASICON materials $Na_3Cr_2(PO_4)_3$ and $Na_3Fe_2(PO_4)_3$, in which the tetravalent cations were completely substituted by Cr^{III} and Fe^{III}, appear to behave differently than the other NASICON materials. Although they have high pre-exponential factors and high activation energies, the ionic conductivity is higher than expected in both cases. They are the only NASICON materials in the literature in which the M cations contain remaining d-electrons in the valence shell. The presence of these electrons seems to have an impact on the crystal structure and the ionic conductivity which still needs to be investigated.

4.3.2. Conduction path

When Hong [9] described the first NASICON, he emphasized the importance of the size of the bottleneck in the conduction pathway of the Na^+ ions. In the NASICON structure, it consists of two triangles which have a common MO_6 octahedral edge. The two MO_6 octahedral vertices defining the distance between both triangle vertices are separated by a PO_4 tetrahedral edge. The positions Na(1) and Na(2) are located above and below the bottleneck, as shown in Fig. 2. Losilla et al. [27] tried to find a direct correlation between the areas T1 and T2 through which the Na^+ ions move and the activation energy. For $Na_{1.4}In_{0.4}M_{1.6}(PO_4)_3$ (M = Ti, Sn, Hf, Zr) such a correlation was found between the area T1 (the smaller triangle) and E_a.

As an effort to extend this observation, the area of triangle T1 was calculated for about 30 NASICON materials for which the complete refined crystal structure is available; the values are listed in Table 5.

The influence of this bottleneck on the activation energy is shown in Fig. 8 and the hypothesis of Losilla et al. is confirmed on a more general basis and wider scale: the activation energy decreases linearly with increasing area T1, i.e. with wider ionic pathway. The result of the linear regression is:

Table 5
Values of the area T1 and the activation energy for different NASICON materials.

NASICON material	Space group	Area T1 [Å^2]	E_a [eV]	Ref.
$NaSnTi(PO_4)_3$	$R\bar{3}c$	4.813	0.62	[25,40,59]
$NaZr_2(PO_4)_3$	$R\bar{3}c$	5.246	0.47	[9]
$NaTi_2(PO_4)_3$	$R\bar{3}c$	4.862	0.62	[26,37,38,60]
$NaSn_2(PO_4)_3$	$R\bar{3}c$	4.983	0.575	[25,39,61]
$NaNbZr(PO_4)_3$	$R\bar{3}c$	5.360	0.54	[28]
$Na_{1.2}In_{0.2}Zr_{1.8}(PO_4)_3$	$R\bar{3}c$	5.203	0.49	[36]
$Na_{1.4}In_{0.4}Ti_{1.6}(PO_4)_3$	$R\bar{3}c$	4.836	0.535	[27]
$Na_{1.4}In_{0.4}Sn_{1.6}(PO_4)_3$	$R\bar{3}c$	4.896	0.53	[27]
$Na_{1.4}In_{0.4}Hf_{1.6}(PO_4)_3$	$R\bar{3}c$	5.111	0.405	[27]
$Na_{1.4}In_{0.4}Zr_{1.6}(PO_4)_3$	$R\bar{3}c$	5.198	0.4	[27]
$Na_{1.4}Al_{0.4}Ti_{1.6}(PO_4)_3$	$R\bar{3}c$	4.739	0.54	[56,57]
$Na_{1.6}Al_{0.6}Ti_{1.4}(PO_4)_3$	$R\bar{3}c$	4.743	0.56	[56,57]
$Na_{1.8}In_{0.8}Zr_{1.2}(PO_4)_3$	$R\bar{3}c$	5.258	0.42	[36]
$Na_{1.8}Al_{0.8}Ti_{1.2}(PO_4)_3$	$R\bar{3}c$	4.714	0.55	[56,57]
$Na_{1.9}Al_{0.9}Ti_{1.1}(PO_4)_3$	$R\bar{3}c$	4.722	0.51	[56,57]
$Na_2InZr(PO_4)_3$	$R\bar{3}c$	5.276	0.39	[36]
$Na_{2.2}In_{1.2}Zr_{0.8}(PO_4)_3$	$R\bar{3}c$	5.191	0.42	[36]
$Na_{2.5}Sc_{0.2}Zr_{1.8}(SiO_4)_{1.3}(PO_4)_{1.7}$	$R\bar{3}c$	5.526	0.3	[58,62]
$Na_{2.6}In_{1.6}Zr_{0.4}(PO_4)_3$	$R\bar{3}c$	5.224	0.46	[36]
$Na_{2.8}In_{1.8}Zr_{0.2}(PO_4)_3$	$R\bar{3}c$	5.241	0.43	[36]
$Na_3Cr_2(PO_4)_3$	$R\bar{3}c$	4.899	0.680	[48,49,54,63]
$Na_3Sc_2(PO_4)_3$	$R\bar{3}c$	5.300	0.508	[22,48,55]
$Na_3Fe_2(PO_4)_3$	$R\bar{3}c$	4.788	0.82	[48,54,64]
$Na_3MgZr(PO_4)_3$	$R\bar{3}c$	5.265	0.410	[65]
$Na_3ScZr(SiO_4)_2(PO_4)$	$R\bar{3}c$	5.380	0.310	[58,62]
$Na_4Zr_2(SiO_4)_3$	$R\bar{3}c$	5.283	0.380	[42,43,66]
$NaGe_2(PO_4)_3$	$R\bar{3}$	4.509	0.81	[26,67]
$Na_{1.13}Al_{0.13}Ge_{1.87}(PO_4)_3$	$R\bar{3}$	4.653	0.63	[56]
$Na_{1.15}Al_{0.15}Sn_{1.85}(PO_4)_3$	$R\bar{3}$	4.625	0.56	[56]
$Na_3Zr_2(SiO_4)_2(PO_4)$	C2/c	5.223	0.33	[9,16,41]
$Na_3Sc_{0.5}Zr_{1.5}(SiO_4)_{1.5}(PO_4)_{1.5}$	C2/c	5.612	0.37	[58,62]
$NaHf_2(PO_4)_3$	$R\bar{3}c$	5.200	0.65	[26,32,38]

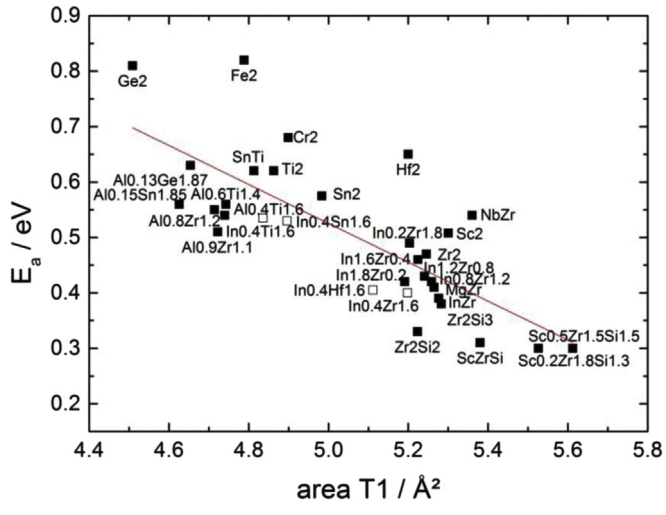

Fig. 8. Dependence of the triangle area T1 on the activation energy. The compositions $Na_{1+2w+x-y+z}M_w^{(II)}M_x^{(III)}M_y^{(V)}M_{2-w-x-y}^{(IV)}(SiO_4)_z(PO_4)_{3-z}$ are labelled $M_w^{(II)}M_x^{(III)}M_y^{(V)}M_{2-w-x-y}^{(IV)}Si_z$, the open symbols represent the materials investigated by Losilla et al. [36]. The line is the result of the linear regression (Eq. (3)).

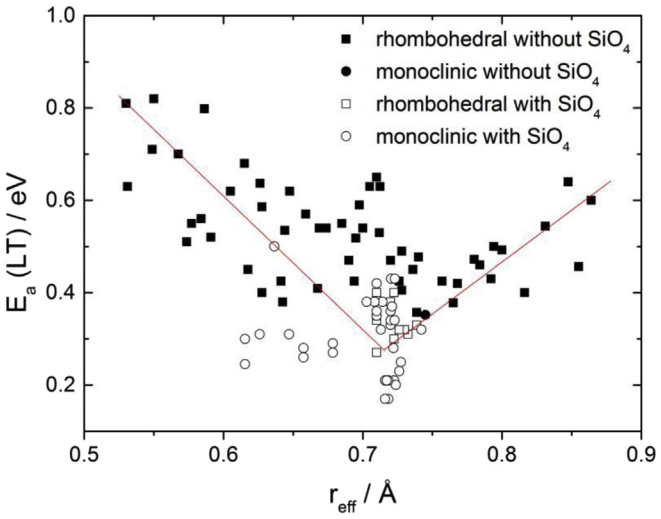

Fig. 10. Low-temperature values of activation energy as a function of the effective ionic radius r_{eff} in $Na_{1+2w+x-y}M_w^{(II)}M_x^{(III)}M_y^{(V)}M_{2-w-x-y}^{(IV)}(PO_4)_3$ (full symbols) and $Na_{1+2w+x-y+z}M_w^{(II)}M_x^{(III)}M_y^{(V)}M_{2-w-x-y}^{(IV)}(SiO_4)_z(PO_4)_{3-z}$ (open symbols) with rhombohedral (■, □) and monoclinic (●, ○) symmetry. The lines are a guide to the eye.

$$E_a = -0.35113 \cdot \text{area}_{T1} + 2.28102; \quad R^2 = 0.56515 \qquad (3)$$

It is interesting to note once again that the compositions with the lowest E_a and largest area T1 are those with partial substitution of P with Si.

The impact of the effective ionic radius r_{eff} on the bottleneck for the Na^+ conduction in these NASICON materials is summarized in Fig. 9. The area T1 increases with an increasing effective ionic radius of the M cations up to a value that is close to the optimal cationic radius of 0.72 Å (see Fig. 3). However, the fact that an optimal r_{eff} exists close to 0.72 Å for the ionic conductivity cannot be clearly observed here because the number of data sets is limited. Although the trend appears to level off at about 0.72 Å for pure phosphate materials, i.e. the area T1 remains constant with increasing r_{eff}, it also shows a steep increase for NASICON materials where P was partially substituted with Si.

The influence of the effective ionic radius r_{eff} on the activation energy is shown in Fig. 10. It confirms the existence of an ideal ionic radius. In addition, the positive impact of the substitution of P with Si is highlighted again (open symbols) and shows that the activation energy can be significantly reduced by changing the central ion of the tetrahedra. An initial explanation for this phenomenon is given in Fig. 10: the introduction of Si in NASICON materials induces a loss of symmetry, i.e. a transition from rhombohedral to monoclinic crystal structure where the sodium ions are more mobile. More structural data on monoclinic NASICON materials could allow this hypothesis to be validated by calculating the area T1 for these materials and correlating it with the activation energy. This would strengthen the data set shown in Fig. 8.

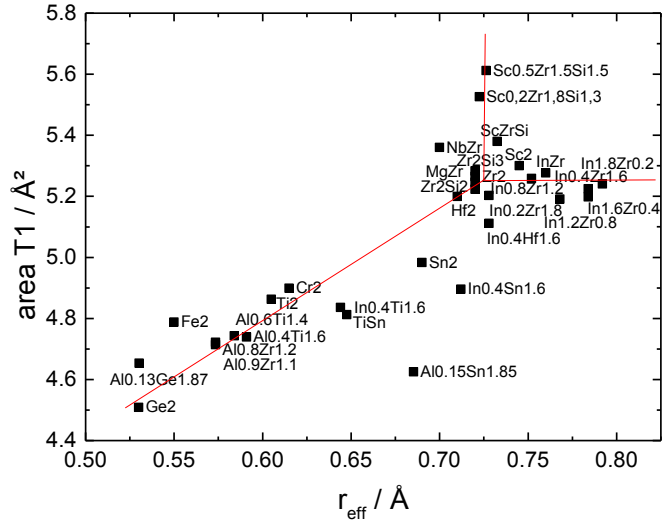

Fig. 9. Dependence of the triangle area T1 on the effective ionic radius. The lines are a guide to the eye.

5. Conclusions

The diversity of NASICON materials and their properties were surveyed and analysed, allowing the identification of the compositional and crystal-chemical criteria leading to a high ionic conductivity by collecting data of transport property and crystal structure of about 110 compositions:

- Optimal amount of charge carriers depending on the composition (around 3.3 mol of Na per formula unit),
- Mean size of the M cations in $Na_{1+2x+y+z}M_x^{(II)}M_y^{(III)}M_{2-x-y}^{(IV)}(SiO_4)_z(PO_4)_{3-z}$ close to 0.72 Å,
- Monoclinic distortion.

These materials have been thoroughly studied in the past 40 years but there are still some open questions worth to be answered to fully understand sodium mobility in this crystal lattice. For example, the influence of the crystal structure (monoclinic distortion) on the size of the bottleneck should be investigated in more detail, because the number of available data sets is rather limited.

Understanding Na^+ mobility in these materials would pave the way towards synthesizing new or improved sodium ion conductors as alternatives to the β-aluminas. In addition, this knowledge could be applied to other ionic conductors with a NASICON structure such as Li^+-ion conductors. Their compositional diversity gives rise to other possible applications, e.g. as cathode material [33,34] or as pigments [35].

References

[1] Z. Yang, J. Zhang, M.C. Kintner-Meyer, X. Lu, D. Choi, J.P. Lemmon, J. Liu, Chem. Rev. 111 (2011) 3577–3613.
[2] H. Ibrahim, A. Ilinca, J. Perron, Renew. Sustain. Energy Rev. 12 (2008) 1221–1250.
[3] V. Palomares, P. Serras, I. Villaluenga, K.B. Hueso, J. Carretero-González, T. Rojo, Energy Environ. Sci. 5 (2012) 5884–5901.
[4] B.L. Ellis, L.F. Nazar, Curr. Opin. Solid State Mater. Sci. 16 (2012) 168–177.
[5] C.A. Beevers, M.A.S. Ross, Z. Kristallogr. 97 (1937) 59–66.
[6] F. Sauvage, L. Laffont, J.M. Tarascon, E. Baudrin, Inorg. Chem. 46 (2007) 3289–3294.
[7] Y. Cao, L. Xiao, W. Wang, D. Choi, Z. Nie, J. Yu, L.V. Saraf, Z. Yang, J. Liu, Adv. Mater. 23 (2011) 3155–3160.
[8] X. Ma, H. Chen, G. Ceder, J. Electrochem. Soc. 158 (2011) A1307–A1312.
[9] H.Y.P. Hong, Mater. Res. Bull. 11 (1976) 173–182.
[10] B.L. Ellis, W.R.M. Makahnouk, Y. Makimura, K. Toghill, L.F. Nazar, Nat. Mater. 6 (2007) 749–753.
[11] K. Zaghiba, J. Trottiera, P. Hovingtona, F. Brochua, A. Guerfia, A. Maugerb, C.M. Julienc, J. Power Sources 196 (2011) 9612–9617.
[12] J. Barkerz, M.Y. Saidi, J.L. Swoyer, Electrochem. Solid State Lett. 6 (2003) A1–A4.
[13] F. Sauvage, E. Quarez, J.M. Tarascon, E. Baudrin, Solid State Ionics 8 (2006) 1215–1221.
[14] N. Recham, J.N. Chotard, L. Dupont, K. Djellab, M. Armand, J.-M. Tarascon, J. Electrochem. Soc. 156 (2009) A993–A999.
[15] F. Lalère, J.B. Leriche, M. Courty, S. Boulineau, V. Viallet, C. Masquelier, V. Seznec, J. Power Sources 247 (2014) 975–980.
[16] H.Y.P. Hong, J.B. Goodenough, J.A. Kafalas, Mater. Res. Bull. 11 (1976) 203–220.
[17] N. Anantharamulu, K.K. Rao, G. Rambabu, B.V. Kumar, V. Radha, M. Vithal, J. Mater. Sci. 46 (2011) 2821–2837.
[18] M.A. Subramanian, R. Subramanian, A. Clearfield, Solid State Ionics 18 & 19 (1986) 562–569.
[19] M. Catti, S. Stramare, R. Ibberson, Solid State Ionics 123 (1999) 173–180.
[20] J.E. Iglesias, J. Sanz, A. Martinez-Juarez, J.M. Rojo, J. Solid State Chem. 120 (1997) 322–326.
[21] E. Dashjav, F. Tietz, Z. Anorg. Allg. Chem. (2014) in press.
[22] G. Collin, R. Comes, J.P. Boilot, P. Colomban, J. Phys. Chem. Solids 47 (1986) 843–854.
[23] A. Ponrouch, E. Marchante, M. Courty, J.M. Tarascon, M.R. Palacín, Energy Environ. Sci. 5 (2012) 8572–8583.
[24] R.D. Shannon, Acta Crystallogr. A32 (1976) 751–767.
[25] J.M. Winand, A. Rulmont, P. Tarte, J. Solid State Chem. 93 (1991) 341–349.
[26] H. Aono, A. Sugimoto, J. Am. Ceram. Soc. 79 (1996) 2786–2788.
[27] E.R. Losilla, M.A.G. Aranda, S. Bruque, A.R. West, Chem. Mater. 10 (1998) 665–673.
[28] L. Bennouna, S. Arsalane, R. Brochu, M.R. Lee, J. Chassaing, M. Quarton, J. Solid State Chem. 114 (1995) 224–229.
[29] M.P. Carrasco, M.C. Guillem, J. Alamo, Solid State Ionics 63/65 (1992) 684–687.
[30] A.R. West, Solid State Chemistry and Its Applications, John Wiley & Sons, Chichester, UK, 1987.
[31] J.B. Goodenough, Annu. Rev. Mater. Res. 33 (2003) 91–128.
[32] E.M. Vogel, R.J. Cava, E. Rietman, Solid State Ionics 14 (1984) 1–6.
[33] K. Trad, D. Carlier, L. Croguennec, A. Wattiaux, B. Lajmi, M.B. Amara, C. Delmas, J. Phys. Chem. 114 (2010) 10034–10044.
[34] K. Saravanan, C.W. Mason, A. Rudola, K.H. Wong, P. Balaya, Adv. Energy Mater. 3 (2013) 444–450.
[35] F.J. Berry, N. Costantini, L.E. Smart, Solid State Ionics 177 (2006) 2889–2896.
[36] E.R. Losilla, M.A.G. Aranda, S. Bruque, A.R. West, Chem. Mater. 12 (2000) 2134–2142.
[37] J.L. Rodrigo, J. Alamo, Mater. Res. Bull. 26 (1991) 475–480.
[38] R.J. Cava, E.M. Vogel, D.W. Johnson, in: Communications of the American Ceramic Society, 1982, pp. C-157–C-159.
[39] M.P. Carrasco, M.C. Guillem, J. Alamo, Solid State Ionics 63/65 (1992) 688–691.
[40] M.P. Carrasco, M.C. Guillem, J. Alamo, Mater. Res. Bull. 28 (1993) 547–556.
[41] A. Ignaszak, P. Pasierb, R. Gajerski, S. Komornicki, Thermochim. Acta 426 (2005) 7–14.
[42] U.V. Alpen, M.F. Bell, H.H. Hoefer, Solid State Ionics 34 (1981) 215–218.
[43] D. Yvanov, J. Currie, H. Bouchard, A. Lecours, J. Andrian, A. Yelon, S. Poulin, Solid State Ionics 67 (1994) 295–299.
[44] W. Wang, Z. Zhang, X. Ou, J. Zhao, Solid State Ionics 28 (1988) 442–445.
[45] T. Takahashi, K. Kuwabara, M. Shibata, Solid State Ionics 1 (1980) 163–175.
[46] F. Krok, D. Kony, J.R. Dygas, W. Jakubowski, W. Bogusz, Solid State Ionics 36 (1989) 251–254.
[47] W. Bogusz, F. Krok, W. Jakubowski, Solid State Ionics 9/10 (1983) 803–808.
[48] J.M. Winaud, A. Rulmont, P. Tarte, J. Mater. Sci. 25 (1990) 4008–4013.
[49] C. Delmas, J.C. Viala, R. Olazcuaga, G.L. Flem, P. Hagenmuller, Solid State Ionics 34 (1981) 209–214.
[50] J.M. Winand, A. Rulmont, P. Tarte, J. Solid State Chem. 87 (1990) 83–94.
[51] M. Nagai, S. Fujitsu, T. Kanazawa, Solid State Ionics 34 (1981) 233–236.
[52] Y. Miyajima, Y. Saito, M. Matsuoka, Y. Yamamoto, Solid State Ionics 84 (1996) 61–64.
[53] Y. Miyajima, T. Miyoshi, J. Tamaki, M. Matsuoka, Y. Yamamoto, C. Masquelier, M. Tabuchi, Y. Saito, H. Kageyama, Solid State Ionics 124 (1999) 201–211.
[54] F. d'Yvoire, M. Pintard-Screpel, E. Bretey, M.d.l. Rochere, Solid State Ionics 9/10 (1983) 851–858.
[55] L. Boehm, C.J. Delbecq, E. Hutchinson, S. Susman, Solid State Ionics 5 (1981) 311–314.
[56] P. Maldonado-Manso, M.A.G. Aranda, S. Bruque, J. Sanz, E.R. Losilla, Solid State Ionics 176 (2005) 1613–1625.
[57] F.E. Mouahid, M. Bettach, M. Zahir, P. Maldonado-Manso, S. Bruque, E.R. Losilla, M.A.G. Aranda, J. Mater. Chem. 10 (2000) 2748–2753.
[58] M.A. Subramanian, P.R. Rudolf, A. Clearfield, J. Solid State Chem. 60 (1985) 172–181.
[59] M.P. Carrasco, M.C. Guillem, J. Alamo, Mater. Res. Bull. 27 (1992).
[60] A. Ivanov, K. Yu, E.L. Belokoneva, E. Tismenko, N.V. Simonov, Dokl. Akad. Nauk. SSSR 252 (1980) 1122–1125.
[61] J.L. Rodrigo, J. Alamo, Mater. Res. Bull. 27 (1992) 1091–1098.
[62] P.J. Squattrito, P.R. Rudolf, P.G. Hinson, A. Clearfield, K. Volin, J.D. Jorgensen, Solid State Ionics 31 (1988) 31–40.
[63] G. Lucazeau, M. Barj, J.L. Soubeyroux, A.J. Dianoux, C. Delmas, Solid State Ionics 18/19 (1986) 959–963.
[64] C. Masquelier, C. Wurm, J.R. Carvajal, J. Gaubicher, L. Nazar, Chem. Mater. 12 (2000) 525–532.
[65] M. Chakir, A.E. Jazouli, D.d. Waal, J. Solid State Chem. 179 (2006) 1883–1891.
[66] J.J. Capponi, J.C. Joubert, R.D. Shannon, J. Solid State Chem. 39 (1981) 219–229.
[67] D. Zhao, Z. Xie, J. Hu, H. Zhang, W.L. Zhang, S.L. Yang, W.D. Cheng, J. Mol. Struct. 922 (2009) 127–134.